JOURNAL OF APPLIED ELECTROCHEMISTRY **28** (1998) 617–622

pH measurement in the vicinity of a cathode evolving hydrogen gas using an antimony microelectrode

T. HONDA, K. MURASE, T. HIRATO, Y. AWAKURA*

Department of Materials Science and Engineering, Kyoto University, Sakyo-ku, Kyoto 6068501, Japan

Received 19 May 1997; revised 18 August 1997

An antimony microelectrode was prepared by quenching a molten Sb–Sb_2O_3 mixture (2% Sb_2O_3). The local pH in the vicinity of a cathode evolving hydrogen gas was directly measured using the microelectrode. The local pH during electrolysis of KCl-glycine aqueous solutions was increased by proton consumption; however, the increment decreased with increasing concentrations of glycine, a buffering agent. The diffusion-limiting current density of hydrogen evolution involving proton reduction was controlled by the concentrations of the proton-donating species: protonated-glycine $^+H_3NCH_2COOH$ and H_3O^+ ions. A plot of the current density against the sum of the concentrations gives a single straight line passing through the origin. The phenomena are discussed in terms of electrodeposition processes of base metals.

Keywords: *antimony electrode*, *microelectrode*, *local pH*, *electrodeposition*, *buffer action*, *diffusion layer*

1. Introduction

Electrodeposition of metals from aqueous solutions is usually affected by the hydrogen ion concentration (pH) of the medium. Evolution of hydrogen gas is more or less inevitable during electrodeposition of base metals such as nickel and zinc. In such cases, the pH in the vicinity of the cathode increases and a metal hydroxide layer forms on the cathode. To avoid the increase in pH various kinds of buffering agents have been tried. However, the amount of buffering agent has been determined only empirically on the basis of deposit quality and current efficiency etc. We studied chromium electrodeposition from divalent chromium electrolyte solutions containing buffering agents such as formic acid, glycine, and citric acid, and found that lustrous chromium deposits were obtained under conditions where hydrogen gas evolution proceeded at a diffusion-limiting current [1, 2]. Thus, it is important to obtain information on the local pH in the vicinity of the cathode, that is, the pH profile across the cathode diffusion layer and also on the relationship between the diffusion-limiting current and the amount of buffering agent, which are closely related to the quality and the current efficiency of the metal deposition.

Attempts have been made to determine a practical pH profile across the cathode diffusion layer using a glass microelectrode [3–6], an antimony microelectrode [7–10] and an optical interferometer [11]. The optical interferometer is not suitable for solutions containing many components. However, the antimony-microelectrode method is most convenient in terms of assembling the electrode.

In the present study, an antimony microelectrode was assembled and pH values in the vicinity of the cathode were measured. Resulting pH profiles across the cathode diffusion layer were discussed in terms of buffer capacity of solutions, which is closely related to simultaneous hydrogen evolution.

2. Experimental setup

Granulated antimony metal was ground in an agate mortar and mixed with powdery antimony(III)oxide Sb_2O_3 (2–10 wt %). The mixture was charged into a Pyrex-glass tube (inner diam. 2 mm) and then allowed to melt using a gas burner with drawing out of the softened glass tube so as to reduce the inner diameter to about 0.5 mm. After quenching, a needle-like solid solution of Sb/Sb_2O_3 was obtained by breaking the glass tube. A coated copper wire was soldered to one end of the Sb_2O_3/Sb needle. An epoxy resin was applied to the whole surface of the Sb_2O_3/Sb needle except the end.

For pH measurements in the vicinity of the cathode surface, the resulting antimony microelectrode (Sb-electrode) was fixed at the tip of a Luggin capillary with a small piece of wedge-shaped silicon rubber. It is important to adjust the end of the Sb-electrode to that of the Luggin capillary in order to exclude potential drop between the cathode and the anode in the bath. The end of the Sb-electrode was cleaned with a silicon-carbide sandpaper (no. 1200) before use. Figure 1 illustrates a cross-section of the tip of the Luggin capillary; around the silicon rubber there is an opening through which electrolyte (i.e. test solution) in and outside the capillary was connected electrically.

*Corresponding author.

0021-891X

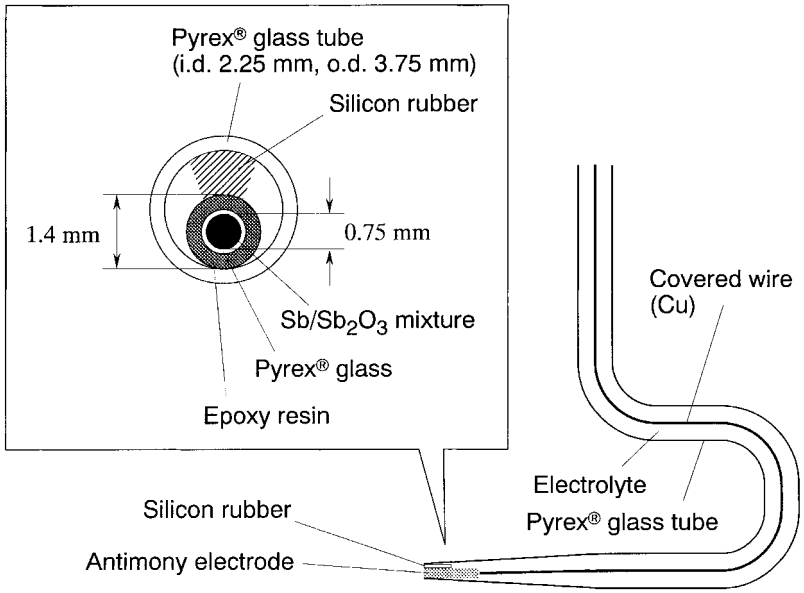

Fig. 1. Cross section of the tip of Luggin capillary with antimony microelectrode.

Figure 2 shows a schematic representation of the bath employed for the measurements of pH in the cathode diffusion layer. A copper disc (diam. 12 mm) and a spiral platinum wire were used as cathode and anode, respectively. The cathode was cemented in an epoxy resin such that one surface, which was polished with 0.1 μm alumina abrasive, was exposed to the test solution. The antimony electrode in the Luggin capillary was kept just in front of the copper cathode using a holder with micrometer so as to measure the distance between the copper cathode surface and the antimony electrode in the range 30 μm to 5 mm. Silver silver chloride (Ag/AgCl) electrodes immersed in 3.3 mol dm^{-3} KCl solution were used as reference electrodes for both the Cu cathode and Sb electrode.

Standard buffer solutions, that is, 0.05 mol dm^{-3} potassium trihydrogen dioxalate dihydrate (pH 1.68 ± 0.02), 0.05 mol dm^{-3} potassium hydrogen phthalate (pH 4.01 ± 0.02), 0.025 mol dm^{-3} potassium dihydrogenphosphate – 0.025 mol dm^{-3} disodium hydrogenphosphate equimolar mixture (pH 6.86 ± 0.02), and 0.01 mol dm^{-3} sodium borate (pH 9.18 ± 0.02), were purchased from Nacalai Tesque Inc. together with other chemicals (acids and salts). Deionized water with electric resistivity of $> 5 \times 10^6\ \Omega$ cm was used to dilute the buffers or to dissolve the chemicals.

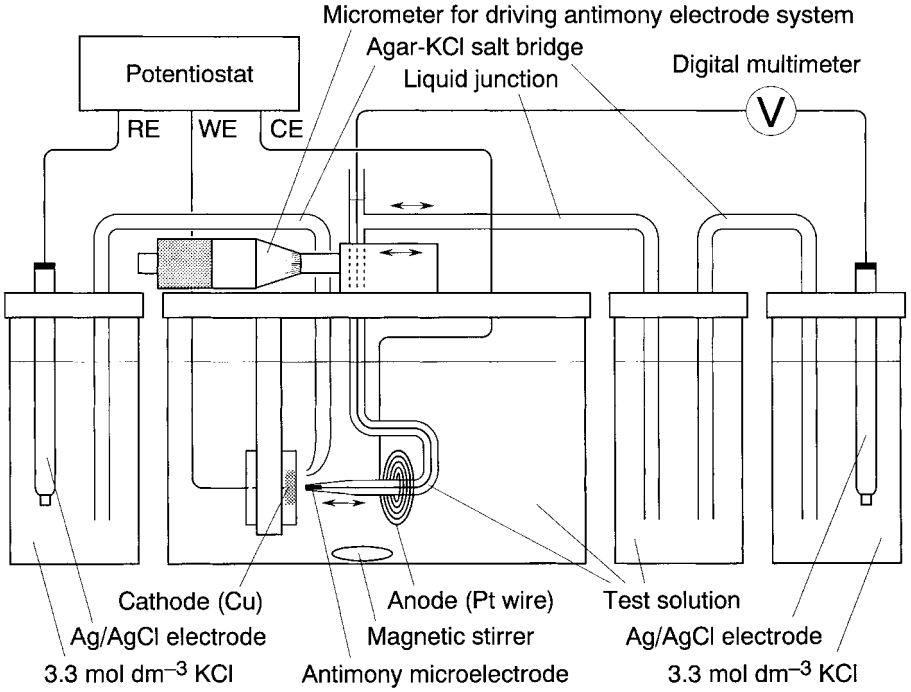

Fig. 2. Schematic representation of the electrolytic bath assembled for measurement of pH in the cathode diffusion layer using an antimony microelectrode.

3. Results

3.1. *Response of antimony microelectrodes*

Mixtures of adequate amounts of standard buffer solutions were used to examine the response of each Sb electrode with Sb_2O_3 contents of 2, 5 and 10%. The electrode potential of Sb electrodes (i.e. Sb_2O_3/Sb mixture) in aqueous solutions is governed by the equilibrium:

$$Sb_2O_3 + 6\,H^+ + 6\,e^- = 2\,Sb + 3\,H_2O \qquad (1)$$

According to thermodynamic data [12] the electrode potential $E_{Sb_2O_3/Sb}$ is calculated as

$$E_{Sb_2O_3/Sb}/V = E^\circ_{Sb_2O_3/Sb} - \frac{0.059}{n}\log\frac{1}{(a_{H^+})^6} = 0.152 - 0.059\,pH \qquad (2)$$

Figure 3 shows a plot of experimentally measured $E_{Sb_2O_3/Sb}$ against pH for Sb-electrode with 2% Sb_2O_3; the pH values were determined using a glass electrode (Horiba 6350-10D) calibrated using standard solutions. Other Sb electrodes with 5 and 10% Sb_2O_3 gave similar plots. For each electrode the plots follow a straight line with smaller slope than that of Equation 2, which is also indicated in the Figure. Intercepts (i.e. $E^\circ_{Sb_2O_3/Sb}$) values, for the experimentally obtained lines are always larger than 0.152 V, the intercept of Equation 2. These differences in the slope and $E^\circ_{Sb_2O_3/Sb}$ may be due to a deviation of activity and chemical potentials of Sb_2O_3 and Sb in the Sb_2O_3/Sb mixture from those for pure substances.

Although the time required to attain a stable Sb-electrode potential increased slightly with increasing Sb_2O_3 content at lower pH, the response time was within 5 min for every electrode and, therefore, subsequent experiments were carried out using an Sb electrode with 2% Sb_2O_3.

Similar $E_{Sb_2O_3/Sb}$ against pH plots were obtained with respect to other buffer solutions, that is hydrogen chloride–potassium chloride, hydrogen chloride–glycine, citric acid–sodium citrate, and acetic acid–sodium acetate mixed solutions. All the above findings indicate that the assembled Sb electrodes can be employed for pH measurements of various aqueous solutions so long as an appropriate $E_{Sb_2O_3/Sb}$ against pH calibration curve is available.

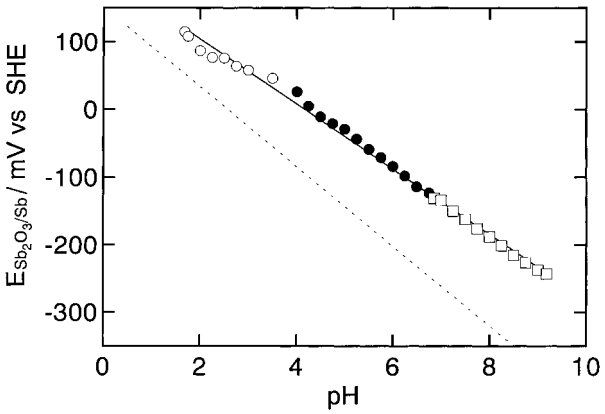

Fig. 3. Relationship between potential of antimony microelectrode (2% Sb_2O_3), $E_{Sb_2O_3/Sb}$, and pH of buffer solutions; the pH was measured with a conventional glass electrode. Dotted line represents calculated potential of antimony microelectrode, assuming that the potential is determined with an equilibrium, $Sb_2O_3 + 6H^+ + 6e^- = 2Sb + 3\,H_2O$.

3.2. *pH measurement in the vicinity of cathode evolving hydrogen*

3.2.1. Selection of weak acid solution. As described above, it is necessary for pH measurements with an Sb electrode, to obtain a calibration curve, that is, a plot of $E_{Sb_2O_3/Sb}$ against pH. If a calibration curve is not available or if the potential of the Sb electrode is not stable in certain solution(s), the method is not suitable for pH measurement. Table 1 summarizes data of calibration curves for various solutions containing potassium chloride (1.0 mol dm^{-3}) and weak acid (0.1–0.5 mol dm^{-3}): glycine, citric acid, or formic acid; the pH of the solutions was adjusted by diluted hydrochloric acid or sodium hydroxide. The calibration curves are found to be linear for each solution, suggesting that all are appropriate for pH measurement with the Sb electrode. The response time of the Sb electrode was fastest and the electrode potential was stable with the potassium chloride–glycine solutions. Therefore, subsequent experiments

Table 1. Relationship between rest potential of antimony microelectrode and pH of electrolyte containing KC1 and weak acid

Electrolyte (1 M = 1 mol dm^{-3})	*pH range*	$E_{Sb_2O_3/Sb}/mV = a + b\,pH$	
		a	*b*
1.0 M KC1	1.57–4.55	180.4 ± 4.1	−37.4 ± 1.7
	4.55–7.42	120.5 ± 2.9	−25.2 ± 1.1
1.0 M KC1–0.1 M glycine	1.86–8.27	201.1 ± 13.6	−45.7 ± 1.8
1.0 M KC1–0.2 M glycine	1.97–8.19	200.6 ± 4.2	−47.2 ± 0.6
1.0 M KC1–0.5 M glycine	1.90–9.00	178.1 ± 8.3	−43.8 ± 1.0
1.0 M KC1–0.1 M citric acid	1.90–8.14	171.8 ± 11.7	−46.9 ± 1.8
1.0 M KC1–0.2 M citric acid	1.71–8.63	172.7 ± 4.3	−46.0 ± 0.5
1.0 M KC1–0.5 M citric acid	1.40–8.36	146.1 ± 15.6	−44.5 ± 2.1
1.0 M KC1–0.1 M formic acid	2.21–9.82	153.0 ± 18.9	−36.4 ± 2.4
1.0 M KC1–0.2 M formic acid	2.05–8.38	166.6 ± 15.1	−40.5 ± 2.3
1.0 M KC1–0.5 M formic acid	1.83–9.33	162.8 ± 18.2	−38.6 ± 2.4

were performed using the potassium chloride–glycine mixed solutions unless otherwise noted.

3.2.2. Cathodic polarization curve of KCl–glycine solutions. Figure 4 depicts cathodic polarization curves of aqueous solutions with pH 2 containing potassium chloride (1.0 mol dm^{-3}) and glycine (0–0.2 mol dm^{-3}). Each polarization curve consists of two cathodic reactions: around −0.3 to −0.8 V and below −1.0 V vs SHE, which are attributed to reduction of protons ($2H^+ + 2e^- \rightarrow H_2$) and water ($2H_2O + 2e^- \rightarrow H_2 + 2OH^-$), respectively. Evidently, the diffusion limiting current for proton reduction increases with increasing glycine content. Glycine acts as a diprotic acid which dissociates as

$$^+H_3NCH_2COOH = {}^+NH_3CH_2COO^- + H^+ \qquad pK_{a1} = 2.35 \qquad (3)$$

and

$$^+NH_3CH_2COO^- = H_2NCH_2COO^- + H^+ \qquad pK_{a2} = 9.78 \qquad (4)$$

where pK_{a1} and pK_{a2} are acid dissociation exponents. The increase in the limiting current suggests that undissociated glycine provides protons to the cathode surface as H_3O^+ ions. This phenomenon was observed for other solutions with pH of 2.4 and 3.0.

3.2.3. pH in the vicinity of the cathode. During electrolysis of the potassium chloride-glycine solutions with pH 2, the pH near the cathode surface is enhanced by the consumption of hydrogen ions. pH profiles across the cathode diffusion layer during potentiostatic electrolysis were obtained with the Sb electrode (Fig. 5).

Cathode potentials examined were −0.6, −0.9, −1.0, and −1.1 V vs SHE with respect to the solution containing only 1.0 mol dm^{-3} potassium chloride (Fig. 5(a)); −0.6 and −0.9 V are the highest and lowest potentials which give a diffusion limiting current for the cathodic reaction, $2H^+ + 2e^- \rightarrow H_2$ (Fig. 4). At potentials of −1.0 and −1.1 V, reduction of water molecules in addition to hydrogen ions occurs. Within the examined range of cathode potential, the pH value at 1.0 mm from the cathode surface was the same as that of the bulk solution (i.e. pH 2.0) which was measured with the conventional glass electrode, indicating that the Sb electrode works normally. An increase in pH can be observed within 0.5 mm from the cathode surface. This suggests that the thickness of the cathode diffusion layer is about 0.5 mm, the same value as estimated using the optical interferometer. The pH profiles during electrolysis at −0.6 and −0.9 V vs SHE were nearly identical; an extrapolation of the profiles gives a value at the cathode surface of around 6, which is four pH units larger than the bulk. When electrolysed at −1.0 V vs SHE, the pH profile at >0.1 mm from the cathode

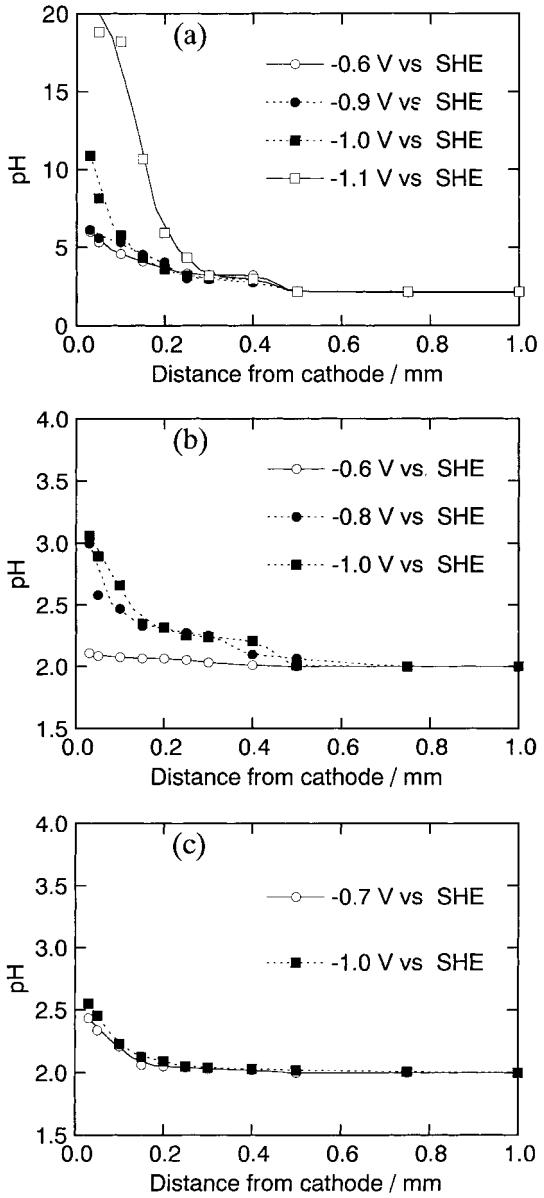

Fig. 5. Profiles of pH across cathode diffusion layer determined by antimony microelectrode during potentiostatic electrolysis of solutions containing KCl (1.0 mol dm^{-3}) and glycine ((a) 0 mol dm^{-3}, (b) 0.1 mol dm^{-3}, and (c) 0.2 mol dm^{-3}); pH of the bulk solution was adjusted with diluted HCl or NaOH aqueous solution.

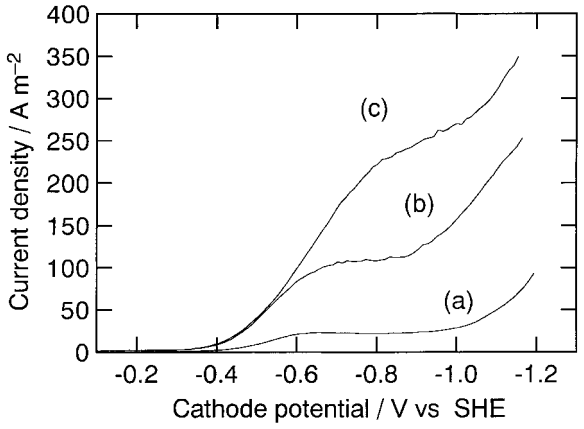

Fig. 4. Cathodic polarization curves of aqueous solutions with pH 2 containing KCl (1.0 mol dm^{-3}) and glycine ((a) 0, (b) 0.1, and (c) 0.2 mol dm^{-3}); pH of the solution was adjusted with diluted HCl or NaOH aqueous solution.

was the same as those observed for −0.6 and −0.9 V vs SHE, whereas the pH within 0.1 mm was larger; the pH at the cathode surface was estimated at about 11. With lower cathode potential, −1.1 V vs SHE, the pH within 0.3 mm of the cathode was increased steeply beyond 14, outside the detection range of the Sb electrode.

For solutions containing 1.0 mol dm^{-3} potassium chloride together with 0.1 and 0.2 mol dm^{-3} glycine, profiles of the pH in the vicinity of the cathode were obtained in the same manner. Evidently, increase of pH toward the cathode surface is depressed, compared with the solution without glycine. At −1.0 V vs SHE, for example, estimated pH values at the cathode surface were 3.1 and 2.6 for the solution with 0.1 and 0.2 mol dm^{-3} glycine, respectively. On the other hand, no difference in the thickness of the cathode diffusion layer was found between the solutions with and without glycine. Consequently, addition of glycine effectively controls the pH within the cathode diffusion layer.

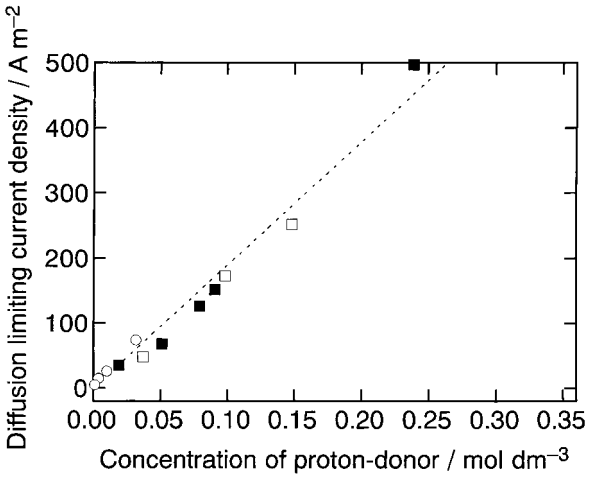

Fig. 6. Relationship between diffusion-limiting current density of reduction of proton and overall content of proton-donating species, $^{+}H_3NCH_2COOH$ and H_3O^{+}. Glycine content: (■) 0.5, (□) 0.2, (■) 0.1 and (○) 0.0 mol dm^{-3}.

4. Discussion

In the presence of glycine, a weak acid, increase in pH in the vicinity of a cathode evolving hydrogen gas was markedly depressed and, further, the diffusion-limiting current density of the cathode reaction, $2H^{+} + 2e^{-} \rightarrow H_2$, increased. These findings indicate that glycine acts as a proton donor against the cathode reaction. These phenomena were observed for all the solutions examined in the pH range 2.0–3.0, where glycine is dissolved as $^{+}H_3NCH_2COOH$ and $^{+}NH_3CH_2COO^{-}$ ions. It can be assumed that only $^{+}H_3NCH_2COOH$ can donate protons to the cathode via Equation 3, because deprotonation of $^{+}NH_3CH_2COO^{-}$ ion hardly takes place due to a large pK_{a2} (= 9.78). Therefore, the diffusion-limiting current density should be determined by both the concentration of protonated glycine, $^{+}H_3NCH_2$-COOH, and 'naked' hydrogen ions. Table 2 summarizes the diffusion-limiting current density together with the concentrations of these species calculated using the acid dissociation exponent, pK_{a1} = 2.35. That a plot of the limiting current density against sum of the concentrations gives a single straight line which passes through the origin (Fig. 6), strongly supports the above assumption.

Electrodeposition processes of base metals from aqueous solutions, such as electrowinning of nickel, are usually performed in the presence of weak acid(s) which have a buffer capacity. The addition of the acid(s) depresses the rise in pH in the vicinity of the cathode and prevents the metal ions forming corresponding hydroxides, which inhibit the reactions on the cathode. However, an oversupply of acid(s) should be avoided, since the acid(s) stimulate hydrogen evolution which lower the cathode current efficiency of metal deposition. Consequently, there is

Table 2. Diffusion limiting current density i_{lim} of cathodic reduction of proton, together with concentrations of protonated glycine and hydrogen ion in buffer solutions under investigation

Solution (1 M = 1 mol dm^{-3})	*pH*	i_{lim}/A m^{-2}	*Concentration of proton donor*/mol dm^{-3}		
			Protonated glycine (**1**)	*Hydrogen ion* (**2**)	**1** + **2**
1.0 M KCl	1.50	74		3.16×10^{-2}	3.16×10^{-2}
	2.00	26		1.00×10^{-2}	1.00×10^{-2}
	2.40	15		3.98×10^{-3}	3.98×10^{-3}
	3.00	5.0		1.00×10^{-3}	1.00×10^{-3}
1.0 M KCl	2.00	126	6.91×10^{-2}	1.00×10^{-2}	7.91×10^{-2}
−0.1 M glycine	2.40	68	4.71×10^{-2}	3.98×10^{-3}	5.11×10^{-2}
	3.00	35	1.79×10^{-2}	1.00×10^{-3}	1.89×10^{-2}
1.0 M KCl	2.00	252	1.38×10^{-1}	1.00×10^{-2}	1.48×10^{-1}
−0.2 M glycine	2.40	173	9.42×10^{-2}	3.98×10^{-3}	9.82×10^{-2}
	3.00	48	3.59×10^{-2}	1.00×10^{-3}	3.69×10^{-2}
1.0 M KCl	2.40	497	2.35×10^{-1}	3.98×10^{-3}	2.39×10^{-1}
−0.5 M glycine	3.00	152	8.95×10^{-2}	1.00×10^{-3}	9.05×10^{-2}

1 $^{+}H_3NCH_2COOH$

an optimum amount of weak acid to be added to electrolytic baths, and the pH measurements with Sb-microelectrode will provide useful information in this respect.

5. Conclusions

The antimony microelectrode is a powerful tool for direct measurement of local pH within the cathode diffusion layer during electrolysis. With regards to the electrolysis of the KCl-glycine solution accompanying hydrogen evolution, increase in pH within the diffusion layer was monitored using the microelectrode; the thickness of the diffusion layer was estimated as about 0.5 mm. Restraint of the pH increment in the presence of glycine, a buffering agent, was also detected, and the phenomenon was discussed in terms of a change in the diffusion-limiting cathodic current of hydrogen reduction.

Studies on the measurement of pH in the vicinity of a cathode during conventional electrochemical processes, such as electroplating of chromium and electrowinning of nickel, are currently under way.

References

[1] T. Hirato, T. Terabatake and Y. Awakura, *in* 'Metallurgical Processes for the Early Twenty-first Century' (edited by H. Y. Sohn), Vol. 1, TMS, Warrendale (1994), p. 975.
[2] T. Hirato, T. Terabatake, E. Watanabe and Y. Awakura, *J. Surf. Finishing Soc. Jpn* **47** (1996) 245.
[3] R. U. Bondar, V. G. Bazdyrev and I. V. Gamali, *J. Appl. Chem. USSR* **46** (1973) 2119.
[4] V. S. Kublanovskii, V. N. Belinskii and D. P. Zosimovich, *Ukrain. Khim. Zhur.* **37** (1973) 713.
[5] V. S. Kublanovskii, G. I. Gushchina and V. S. Kolevatova, *ibid.* **40** (1974) 85.
[6] O. B. Izbekova, V. V. Chelikibi, V. N. Belinskii, *ibid.* **41** (1975) 1321.
[7] J. Matulis and R. Slizys, *Electrochim. Acta* **9** (1964) 1177.
[8] L. A. Golubkov and B. P. Yur'ev, *J. Appl. Chem. USSR* **47** (1974) 74.
[9] K. Higashi, H. Fukushima, T. Urakawa, T. Adaniya and K. Matsudo, *J. Electrochem. Soc.* **128** (1981) 2081.
[10] Y. Lin, T. Ogai, T. Akiyama, H. Fukushima, Y. Yamauchi, *J. Surf. Finishing Soc. Jpn* **47** (1996) 868.
[11] Y. Awakura and Y. Kondo, *J. Electrochem. Soc.* **123** (1976) 1184.
[12] M. Pourbaix, 'Atlas of Electrochemical Equilibria in Aqueous Solutions', Pergamon Press, Oxford (1966), p. 524.